

RESEARCH ARTICLE

Zebrafish *foxc1a* drives appendage-specific neural circuit development

Santanu Banerjee¹, Katharina Hayer², John B. Hogenesch² and Michael Granato^{1,*}

ABSTRACT

Neural connectivity between the spinal cord and paired appendages is key to the superior locomotion of tetrapods and aquatic vertebrates. In contrast to nerves that innervate axial muscles, those innervating appendages converge at a specialized structure, the plexus, where they topographically reorganize before navigating towards their muscle targets. Despite its importance for providing appendage mobility, the genetic program that drives nerve convergence at the plexus, as well as the functional role of this convergence, are not well understood. Here, we show that in zebrafish the transcription factor *foxc1a* is dispensable for trunk motor nerve guidance but is required to guide spinal nerves innervating the pectoral fins, equivalent to the tetrapod forelimbs. In *foxc1a* null mutants, instead of converging with other nerves at the plexus, pectoral fin nerves frequently bypass the plexus. We demonstrate that *foxc1a* expression in muscle cells delineating the nerve path between the spinal cord and the plexus region restores convergence at the plexus. By labeling individual fin nerves, we show that mutant nerves bypassing the plexus enter the fin at ectopic positions, yet innervate their designated target areas, suggesting that motor axons can select their appropriate fin target area independently of their migration through the plexus. Although *foxc1a* mutants display topographically correct fin innervation, mutant fin muscles exhibit a reduction in the levels of pre- and postsynaptic structures, concomitant with reduced pectoral fin function. Combined, our results reveal *foxc1a* as a key player in the development of connectivity between the spinal cord and paired appendages, which is crucial for appendage mobility.

KEY WORDS: Zebrafish, Limb motor neuron, Motor axon, Plexus, Fin nerves, *Foxc1a*, Pectoral fin, Axon guidance

INTRODUCTION

During development, the fidelity with which connections between spinal motor neurons and their appropriate limb muscle targets form is paramount for precise and coordinated motor behaviors. Motor neurons express specific set of guidance receptors that ensure correct navigation at intermediate targets where growth cones select a path towards their appropriate final synaptic targets. For example, after exit from the spinal cord, limb-innervating motor axons avoid a path towards dorsal axial muscles, and instead extend ventrally towards an intermediary target at the base of the limb. Here, motor axons from adjacent spinal cord segments converge and re-organize to innervate their final limb muscle targets. This intermediate target, the plexus, is

considered crucial for proper target innervation, in part because here axons make their final navigational decisions, and are able to compensate for previous migration errors (Ferguson, 1983; Ferns and Hollyday, 1993; Lance-Jones and Landmesser, 1981; Tosney and Landmesser, 1984). For example, rotating spinal cord segments along the anterior posterior axis causes limb nerves to approach the plexus from inappropriate directions, yet compensatory changes within the plexus are thought to correct target innervation (Lance-Jones and Landmesser, 1981). Similarly, following dorsoventral rotation of the limb bud, innervating motor axons also adjust their trajectories in the plexus accordingly, suggesting involvement of local guidance cues within the plexus and in the developing limb (Ferguson, 1983; Tosney and Landmesser, 1984). Combined, these experiments suggest that axonal migration through the plexus area contributes to proper target innervation; however, this has not been tested directly by examining synaptic target selection of axons that bypass the plexus and enter the limb at ectopic locations.

Studies in chick and mouse have revealed that motor neurons express a specific set of cell-adhesion molecules and guidance receptors that are crucial to steer limb motor axons from the limb plexus to target muscles (Bonanomi and Pfaff, 2010; Tang et al., 1992, 1994). For example, motor neurons expressing EphA4 are repelled by ephrin A proteins expressed in the ventral limb mesenchyme and innervate the dorsal limb (Eberhart et al., 2000, 2002; Kania and Jessell, 2003; Luria et al., 2008). By contrast, neuropilin 2 receptor-expressing motor neurons are repelled by the semaphorin 3F ligand expressed in the dorsal limb, and innervate the ventral limb. Similarly, neuropilin 1/semaphorin 3A signaling regulates multiple aspects of limb nerve guidance, including axon fasciculation, timing of entry into the plexus and bifurcation of nerves into dorsal and ventral limb (Huber et al., 2005). Despite this, the genetic program that ensures the convergence of multiple appendage innervating spinal nerves at the plexus, and the significance of this nerve convergence for the innervation pattern and function of vertebrate appendages, is not well understood.

Similar to tetrapods, zebrafish spinal nerves that innervate the pectoral fins, equivalent to the tetrapod forelimbs, converge at base of the pectoral fins to form a plexus before entering their distinct target areas in the fin. Importantly, fin muscle innervation is highly stereotyped (Ma et al., 2010; Thorsen and Hale, 2007), providing an excellent model system with which to determine whether the convergence of spinal motor nerves at the plexus is a prerequisite for proper fin innervation and function, and to identify key players selectively required for the development of the neural circuitry critical for the mobility of vertebrate appendages. Using a combination of forward genetics and whole-genome sequence analysis, we first report on a mutant we isolated in a forward genetic screen based on aberrant projections of fin-innervating motor nerves, and we demonstrate that this mutant phenotype is caused by a presumptive null mutation in the *foxc1a* transcription factor. We show that *foxc1a* is required selectively for pectoral fin-innervating motor axons to converge at the plexus, and

¹Department of Cell and Developmental Biology, University of Pennsylvania Perelman School of Medicine, Philadelphia, PA 19104, USA. ²Department of Pharmacology and Institute for Translational Medicine and Therapeutics, University of Pennsylvania Perelman School of Medicine, Philadelphia, PA 19104, USA.

*Author for correspondence (granatom@mail.med.upenn.edu)

that nerve convergence requires *foxc1a* function in somitic muscle cells located along the nerve path. Moreover, we find that *foxc1a* mutant nerves that bypass the plexus still target their original target area within the fin, providing compelling evidence that convergence of fin nerves at the plexus is not a prerequisite for fin muscle target selection. Finally, we show that despite proper target selection, *foxc1a* mutants exhibit reduced fin innervation, concomitant with a reduction in the amplitude and frequency of fin movement in *foxc1a* mutants. Thus, *foxc1a* is part of a genetic program dedicated to connect spinal cord neurons with their paired appendage synaptic targets to generate appendage mobility.

RESULTS

p162 mutants display pioneering motor axon guidance defects in anterior somite segments

In an antibody-based forward genetic screen (Birely et al., 2005), we identified a mutant, *p162*, with severe axon guidance defects selective for anterior somitic segments. In zebrafish, motor axons navigating through the four anterior somatic segments form the four segmental fin innervating spinal motor nerves, whereas those navigating through more posterior segments innervate exclusively axial trunk muscles (Fig. 1A; Myers et al., 1986; Thorsen and Hale, 2007). By 26 h post-fertilization (hpf) the first motor axons to pioneer into the periphery, the primary motor axons, have exited the spinal cord, and have extended to the most ventral aspect of the myotome (Fig. 1A,B,D; Myers et al., 1986). Although migration of primary motor axons in posterior segments (segments 7–14) of *p162* mutants (hence forth referred as *foxc1a^{p162}*) was indistinguishable from that in wild-type siblings (Fig. 1C, *n*=160 hemisegments in 30 embryos), migration through the anterior segments was severely compromised. Specifically, the majority of anterior primary motor axons in segments 1–6, stalled near or at their first intermediate target, the horizontal myoseptum (Fig. 1E, *n*=165/180 hemisegments in 30 embryos; supplementary material Fig. S1). Although axons in segments 1–4 were affected in all mutant embryos, we noticed that those in segments 5 and 6 were not affected in all embryos, suggesting some degree of phenotypic variability.

To exclude the possibility that the observed axonal defects were secondary, i.e. due to defective somite development, we examined adaxial muscle cell specification, somite polarity and muscle fiber differentiation, as defects in these processes are known to impair motor axon guidance (Birely et al., 2005; Zeller et al., 2002). Antibody staining revealed that adaxial muscle cell numbers, their specification, as well as somite polarity is unaffected in *p162* mutants (Fig. 1F,G; supplementary material Fig. S2). Finally, we examined postsynaptic differentiation as a hallmark of muscle fiber differentiation. Primary motor axons form stereotypic en passant neuromuscular synapses, characterized by the accumulation of acetylcholine receptor (AChR) clusters, at the center of muscle fibers (Fig. 1H; Westerfield et al., 1986). In *p162* mutants, en passant synapses properly localized in the center of muscle fibers, along the entire length of their shortened motor axons (Fig. 1I), suggesting that in *p162* mutants the muscle intrinsic mechanisms crucial for postsynaptic specialization are operational. Taken together, we have identified a mutation in a gene specifically required for motor axon guidance through anterior somite segments.

The *p162* phenotype is caused by a premature stop codon in *foxc1a*

To identify the gene disrupted by the *p162* mutation, we applied a combination of positional cloning and whole-genome sequence

analysis. In brief, we first used genetic linkage analysis via microsatellite mapping to position the *p162* mutation within a 2 Mb interval on chromosome 2, and then performed whole-genome sequencing analysis. Sequence data was aligned to the Zv9/danRer7 genome (UCSC), and then processed through the GATK pipeline (DePristo et al., 2011; McKenna et al., 2010; Van der Auwera et al., 2013). Within the 2 Mb interval defined by genetic mapping, this revealed a unique ‘deleterious’ single nucleotide polymorphism (SNP) (Fig. 2A,B). This SNP was considered ‘deleterious’ because it changes a conserved tryptophan to a premature stop codon in the *foxc1a* gene (W118*; Fig. 2A,B). The zebrafish *foxc1a* gene encodes a 476 amino acid protein, which is 63% identical to the human and mouse FoxC1 homologs. FoxC1 proteins belong to the forkhead family of transcription factors characterized by the forkhead domain consisting of two DNA-binding wing helix domains, crucial for FoxC1 function (Murphy et al., 2004; Nishimura et al., 2001; Saleem et al., 2004; Weisschuh et al., 2006). The *p162* mutation W118* truncates the open reading frame in the forkhead domain (amino acids 72–163). Consistent with previously described morpholino knockdown phenotypes, *foxc1a*

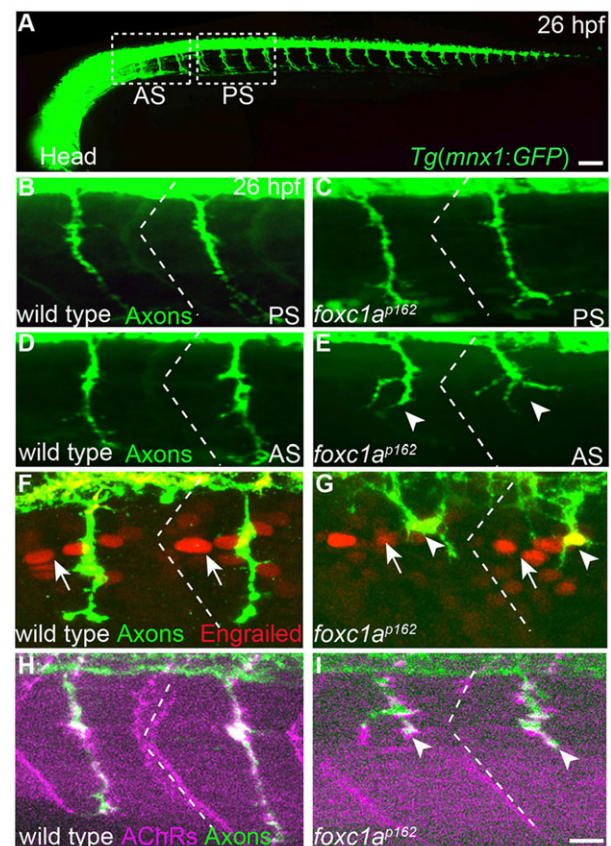


Fig. 1. *foxc1a* guides primary motor axon selectively in anterior somite segments. (A) Lateral (composite) view of a 26-h-old Tg (*mnx1:GFP*) embryo expressing GFP in all motor neurons. White dashed boxes mark anterior somite segments (AS) and posterior segments (PS) considered in this study. Compared with wild type (B,D), *foxc1a* mutants (C,E) exhibit motor axon guidance defects selectively in anterior but not posterior somitic segments. (F–I) Somite polarity (F,G), as revealed by the localization of Engrailed-positive nuclei (arrows) towards the anterior somite boundary (dashed lines), and muscle differentiation (H,I), as revealed by the apposition of muscle AChRs with axons to form en passant synapses are unaffected in *foxc1a* mutants. Arrowheads indicate stalled and branched axons. Scale bars: 50 μ m in A; 10 μ m in B–I.

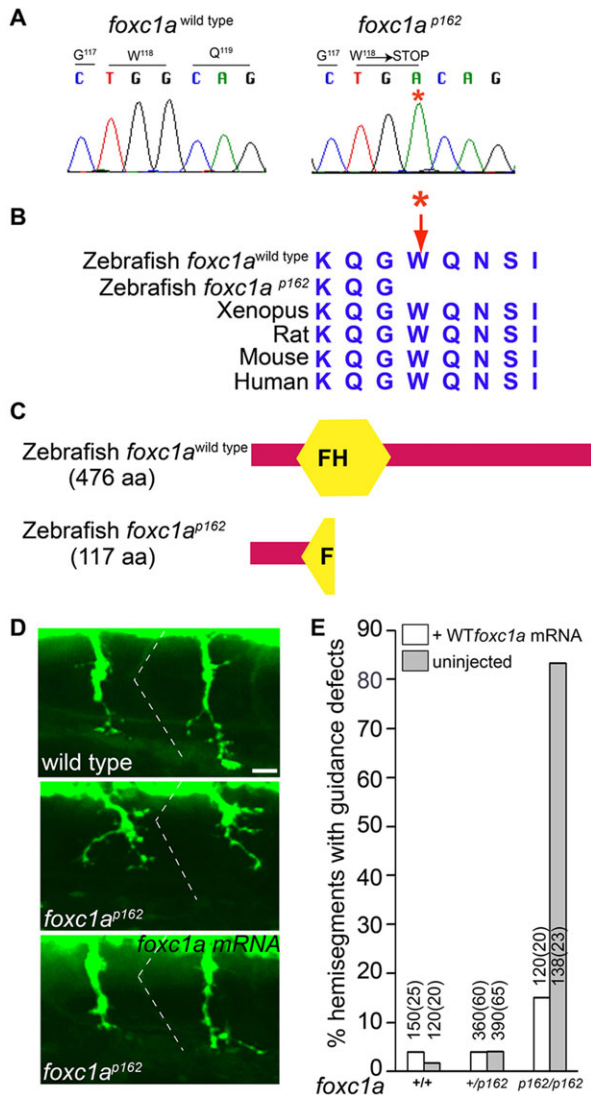


Fig. 2. The p162 mutant phenotype is caused by a nonsense mutation in the *foxc1a* gene. (A,B) The G to A nucleotide mutation converts tryptophan at position 118 into a premature stop codon. (C) Conceptual translation of the *foxc1a*^{p162} predicts a 117 amino acid protein truncated within the forkhead (FH) domain. (D) Injection of wild-type *foxc1a* mRNA restores axon guidance in *foxc1a* mutants. (E) Quantification of the mRNA rescue. Numbers on top of individual bars indicate the number of hemisegments and embryos (brackets) analyzed. For all genotypes, only the first six anterior segments were analyzed. Scale bar: 10 μ m in D.

mutants eventually develop small eyes, pericardial edema and circulation blockage (data not shown; Skarie and Link, 2009; Veldman and Lin, 2012).

To demonstrate that the mutation in the *foxc1a* gene is causative of the observed axon guidance defects, we performed mRNA rescue experiments. For this, we injected mRNA encoding wild-type *foxc1a* and truncated *foxc1a*^{p162} allele (see Materials and Methods) into wild-type and mutant embryos, and examined axonal projection pattern of spinal motor axons at 28 hpf. Injection of wild-type *foxc1a* mRNA into wild-type or sibling embryos did not affect motor axon guidance (quantified in Fig. 2E). Importantly, injection of wild-type *foxc1a* mRNA into mutant embryos restored motor axon guidance (Fig. 2D,E), providing compelling evidence that the p162 mutant phenotype is caused by mutations in the *foxc1a* gene. Injection of mutant *foxc1a* ^{Δ 118-476} mRNA into wild-type or

sibling embryos did not affect axonal projection nor did it rescue axon guidance defects in *foxc1a* mutants, even when injected at 10-fold higher levels than wild-type *foxc1a* mRNA (sufficient to rescue *foxc1a* mutants), consistent with the idea that *foxc1a*^{p162} represents a presumptive null allele ($n=48$ hemisegments in eight embryos for each genotype, data not shown). To our knowledge this is the first evidence for a role for *foxc1a* in motor axon guidance.

***foxc1a* is required for pectoral fin nerve guidance**

Given the role of *foxc1a* in guiding pioneering primary motor axons, we examined the projection patterns of later developing secondary motor axons, which extend along the same path to reach their peripheral targets, yet largely independent of primary motor axons (Myers, 1985; Pike et al., 1992). In somitic segments 5-36, 60-80 secondary motor axons from each spinal cord segments bundle together to form spinal nerves that innervate trunk muscle (Fig. 3A,B). In *foxc1a* mutants, motor nerves innervating trunk muscles appear indistinguishable from those in wild type (Fig. 3A-C; $n=120$ hemisegments in 20 embryos), suggesting that *foxc1a* is dispensable for the guidance of trunk innervating motor nerves. By contrast, in *foxc1a* mutants, pectoral fin-innervating nerves displayed severe defects. Wild-type pectoral fins are innervated by a set of four segmental spinal motor nerves, extending through the four anterior-most somites (Fig. 3A,D,F,H,J). By 48 hpf, nerves 1-3 have converged at the plexus located at the base of the fin, and have just entered the dorsal aspect of the fin (Fig. 3D,F, arrowheads). Nerve 4, without entering the plexus, enters the fin at the ventral aspect (Fig. 3D,F, arrows). In *foxc1a* mutants, the fourth nerve completes migration through the axial myotome, stalls before reaching the ventral extent of the fin but eventually enters the fin (Fig. 3E,G, arrows; Fig. 3I-K). Nerves 1-3 in *foxc1a* mutants fail to converge at the base of the fin plexus (Fig. 3E,G, arrowheads), and instead made contacts with each other at ectopic locations (cyan asterisks in Fig. 3E,G, $n=115/132$ hemisegments in 33 embryos). For example, the third nerve frequently contacted the second or the fourth fin nerve at ectopic locations, from where they extended further ventrally, bypassing the plexus ($n=115/132$ nerves in 27/33 embryos; cyan asterisks in Fig. 3E,G). Furthermore, within individual nerves, motor axons defasciculated and extended along ectopic trajectories (Fig. 3E,G, red asterisks). To determine whether axonal guidance defects result in motor neuron death, we examined motor neuron cell death by TUNEL staining around 48 hpf. Identical to the situation in wild-type embryos, motor neuron death in *foxc1a* mutants was undetectable (supplementary material Fig. S3).

Finally, to determine whether those nerves bypassing the plexus area were ultimately able to enter the fin, we examined fin innervation at later stages. At 96 hpf, *foxc1a* mutant nerves still exhibited ectopic fasciculation with other nerves (Fig. 3I-K), yet were able to enter the pectoral fin, albeit mutant fins displayed a significant reduction in the number of terminal axonal arbors (Fig. 3H-K; and below, see Fig. 6). Combined, our data demonstrate that although *foxc1a* is dispensable for the projection of trunk innervating motor nerves, it is required for the convergence of fin innervating nerves at the fin plexus.

***foxc1a* acts cell non-autonomously in somitic muscle**

To determine how *foxc1a* regulates fin nerve guidance, we examined *foxc1a* mRNA expression at the time of pectoral fin innervation (see Fig. S4 in the supplementary material). At 40 hpf, *foxc1a* expression is enriched in the ventral region of those anterior somite segments through which the first three fin nerves migrate (Fig. 4A-F). Thus,

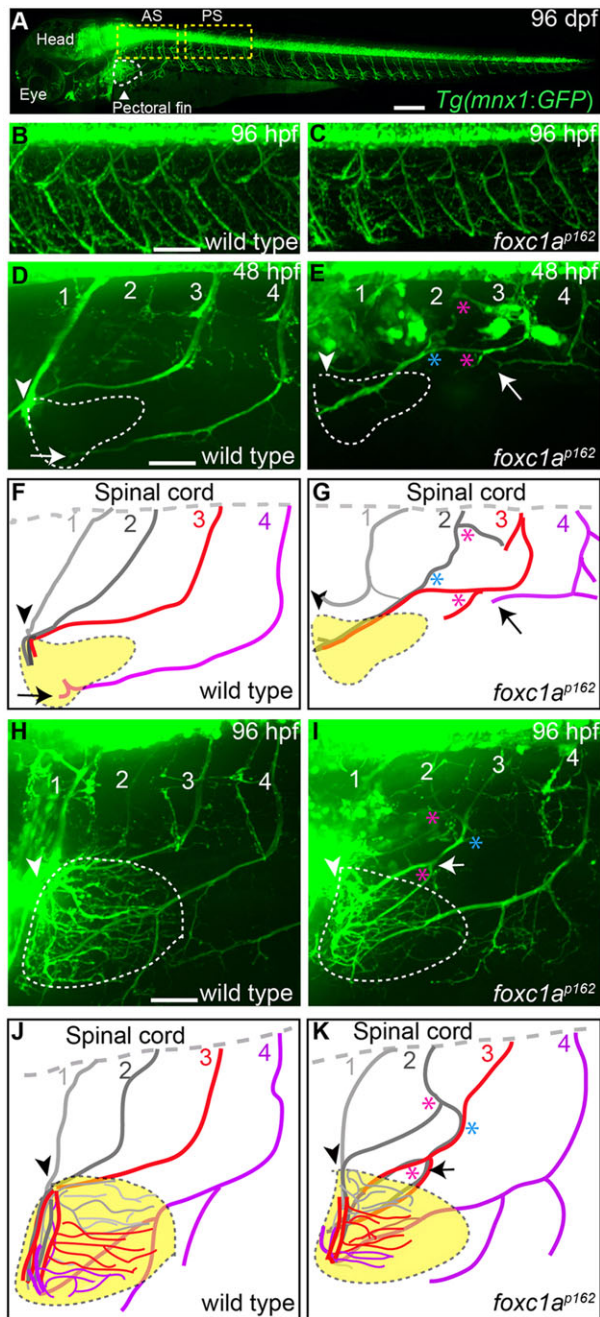


Fig. 3. *foxc1a* is required for fin-innervating motor nerves to convert at the plexus. (A) Lateral (composite) view of a 96-hpf-old *Tg(mnx1:GFP)* larvae expressing GFP in all motor nerves. Yellow dashed boxes mark anterior segments (AS) and posterior segments (PS) considered in this study; white dotted area outlines the pectoral fin. (B,C) Compared with wild-type larvae, trunk innervation (posterior segments) is unaffected in *foxc1a* mutants. (D-G) By contrast, three out of the four fin-innervating nerves in *foxc1a* mutants display axonal defects at 48 hpf (D-G) and at 96 hpf (H-K). Dotted areas outline the pectoral fin, arrowheads indicate the position of the fin plexus and arrows indicate the fourth pectoral fin nerve. Cyan asterisks indicate ectopic fasciculation; red asterisks mark defasciculation. Scale bars: 50 μ m.

consistent with the pectoral fin-innervating nerve defects, we find that *foxc1a* mRNA is expressed at the time when motor axons navigate towards the plexus region, and along their path. We therefore tested whether *foxc1a* functions in somitic muscles to guide fin nerves. To test this we expressed wild-type *foxc1a* under the control of a muscle-specific promoter (*α -actin:foxc1a-p2a-*

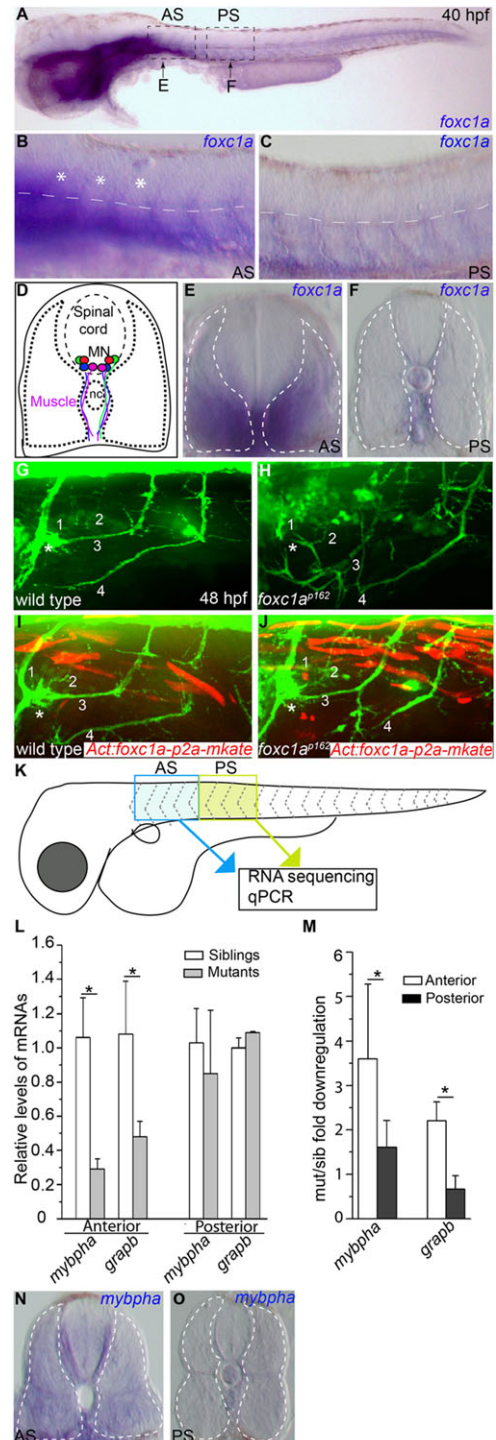


Fig. 4. *foxc1a* is expressed and functions in somitic muscle to guide fin nerves. (A-C) At 40 hpf, *foxc1a* mRNA is highly enriched in anterior (A,B) but not posterior somite segments (A,C). (B,C) Magnified views of anterior and posterior somitic segments shown in A, asterisks indicate the anterior most three segments. (D-F) Cross-sections through anterior and posterior segments (at the level of arrows in A) reveal *foxc1a* mRNA accumulation in muscle fibers located along the fin nerve path. (G-J) Stochastic expression of a *foxc1a-p2a-mKate* transgene in muscle fibers (I,J) restores fin nerve guidance. (K-O) RNA-seq identifies transcripts selectively enriched in anterior segments and downregulated in *foxc1a* mutants, as confirmed by real-time PCR experiments (L,M; asterisks indicate significance; $P < 0.05$, Student's *t*-test) and by *in situ* hybridization of *mybpha* (N, cross-section through anterior segment; O, cross-section through posterior segment). Data are means \pm s.e.m.

mKate) in *foxc1a* mutants. Sparse transient expression of this *foxc1a-p2a-mKate* transgene in only one or two *foxc1a* mutant muscle cells adjacent or underneath the fin nerve path was insufficient to restore axonal guidance or plexus formation ($n=4$ embryos; data not shown and supplementary material Table S1). Only in a small subset of *foxc1a* mutant embryos in which each of the four anterior somite segments contained four to eight *foxc1a-p2a-mKate* transgene-expressing muscle cells adjacent or underneath the fin nerve path did we observe rescue of both nerve migration and convergence at the plexus (Fig. 4J, $n=4$ embryos from a total of 70 mutants containing *foxc1a-p2a-mKate*-positive muscle cells). Conversely, transient transgenic expression of *foxc1a* in motor neurons was unable to restore axon guidance defects ($n=12$ motoneurons in five embryos; data not shown and supplementary material Table S1). Thus, *foxc1a* expression in muscle cells adjacent to the path of each fin innervating nerve is sufficient for fin innervating nerves to converge at the fin plexus, consistent with the idea that *foxc1a* influences the local nerve environment.

foxc1a encodes a transcriptional activator, and based on its expression and requirement in somitic muscles, one possible mechanism by which *foxc1a* might direct fin nerves is by regulating the expression of axonal guidance cues. To determine the complement of *foxc1a*-dependent transcripts specific to the region through which the fin innervating nerves migrate, we performed RNA-seq. Specifically, we isolated wild-type and *foxc1a* mutant tissue samples from anterior somitic segments (AS) through which the fin nerves migrate, and compared those with tissue samples from adjacent posterior segments (PS) devoid of fin-innervating nerves (Fig. 4K; for details, see the Materials and Methods). Importantly, we collected the tissues at 38 hpf, as fin-innervating nerves complete their migration through the somitic compartment.

Given that *foxc1a* acts predominantly as a transcriptional activator and that loss of *foxc1a* selectively affects anterior segment nerves, we focused the RNA-seq analysis on transcripts/genes that were downregulated in *foxc1a* mutants (see supplementary material Table S2 for a complete list of all up- and downregulated transcripts). Comparing wild-type AS and PS RNA-seq profiles with each other and with wild type and *foxc1a* mutants, we identified 12 genes with significantly elevated mRNA levels in wild-type AS compared with wild-type PS, and with reduced levels in *foxc1a* AS profiles compared with wild-type AS profiles (over twofold; supplementary material Table S2). To validate these results, we selected two of these mRNAs and performed real-time PCR analysis as well as *in situ* hybridization. This confirmed that mRNA expression levels of these two genes, *mybpha* (*myosin binding protein H a*) and *graph* (*Grb2-related adaptor protein b*), are significantly downregulated in *foxc1a* anterior somitic segments, confirming that our differential RNA-seq approach can identify *foxc1a*-dependent transcripts enriched in the anterior somitic segments (Fig. 4L–O). Finally, we analyzed the RNA-seq data sets for mRNAs encoding classical axon guidance genes. Among 116 mRNAs expressed in AS samples and associated with the GO term ‘axon guidance’ (<http://www.geneontology.org/>) only *foxd5* mRNAs levels were over twofold reduced in *foxc1a* AS profiles. Although *foxd5* promotes expression of ectoderm specific markers through Notch signaling, a direct role for *foxd5* in axon guidance has not been established (Yan et al., 2009). Thus, while *foxc1a* controls restricted expression of a small set of genes in anterior segments, loss of *foxc1a* does not overtly change the transcriptional profile of axonal guidance genes in these segments.

***foxc1a* function is dispensable for fin target area selection**

In wild-type animals, nerves 1–3 stereotypically converge at the plexus before they enter the fin and innervate their synaptic muscle targets. To determine whether this convergence is important for synaptic target selection in the fin, we examined the innervation pattern of individual *foxc1a* mutant nerves. We focused on the fourth nerve, which is unaffected in *foxc1a* mutants, and on the third nerve, which in *foxc1a* mutants bypasses the plexus and enters the fin at an ectopic position (Fig. 3J,K). To visualize the trajectory of individual nerves, we generated a stable transgenic line [*Tg(mnx1:Kik-GR)*] and photoconverted (green to red) motor neurons expressing the photoconvertible Kik-GR protein. Photoconverting motor neurons contributing to the fourth fin nerve (pseudocolored in magenta) enabled us to visualize the trajectories of many axons within this nerve, as they entered the fin at the ventral aspect and occupied their stereotyped domain restricted to the ventroposterior region of the fin (Fig. 5A,C; $n=4/4$ in four embryos). Although the branch density as well as the total area covered by these axons was reduced in *foxc1a* mutants (see below, Fig. 6), there was no significant difference between wild type and *foxc1a* mutants regarding the territory occupied by fourth-nerve axons (Fig. 5B,D; $n=7/7$ in seven embryos).

Photoconversion of the third nerve confirmed that in *foxc1a* mutant axons enter the fin at an ectopic, ventral position (Fig. 5E–H, arrowheads, $n=5/7$ in seven embryos). Despite their ectopic entry, third-nerve axons mostly innervated their nerve specific fin territory, with only few axons projecting to ectopic sites (Fig. 5E–H). Thus, pectoral fin-innervating axons can select their original fin target areas independently of their prior pathfinding history. This strongly suggests that the mechanisms that control synaptic target innervation in the fin operate independently of those required for appropriate plexus formation and entry into the fin.

***foxc1a* mutants display reduced fin nerve branching and synapse formation**

Although *foxc1a* pectoral fin nerves innervate their appropriate territories, we asked whether the levels of axonal branching and synapse formation are affected. *foxc1a* mutants develop large pericardial edemas and die between 6 and 8 dpf. We therefore performed our analysis on 4-dpf (96 hpf) animals. Immunohistochemistry using the MF20 skeletal muscle myosin-specific antibody (Patterson et al., 2008) did not reveal any significant differences in pectoral fin muscle morphology or total fin muscle area when compared with wild type, suggesting that in *foxc1a* mutants fin muscles are properly differentiated (Fig. 6A–C; $n=7$ fins in seven embryos). Image analysis (for details, see Materials and Methods) revealed that in wild-type embryos ~35% of the total fin muscle territory is occupied by thin axonal branches (Fig. 6D,F, $n=7$ fins). By contrast, *foxc1a* mutant nerves are less branched and occupied ~20% area of the pectoral fin muscles (Fig. 6E,F, $n=7$ fins in seven embryos; for details on quantification, see Materials and Methods). Finally, we used α -bungarotoxin to quantify postsynaptic AChR clusters in pectoral fin muscles (Thorsen and Hale, 2007). In *foxc1a* mutants, AChRs were associated with presynaptic axonal branches (Fig. 6G–K), suggesting that mutant fin muscles have retained their ability to cluster AChRs. To quantify synapses between wild-type and mutant fin, we considered individual AChR cluster juxtaposed to an axon branch as individual synaptic contact sites. This revealed that compared with wild-type animals, the total number of synaptic contact sites in *foxc1a* mutant fins is reduced to about 66% (Fig. 6I). Thus, in *foxc1a* mutants, fin innervating axons target their proper synaptic territories, albeit in reduced numbers.

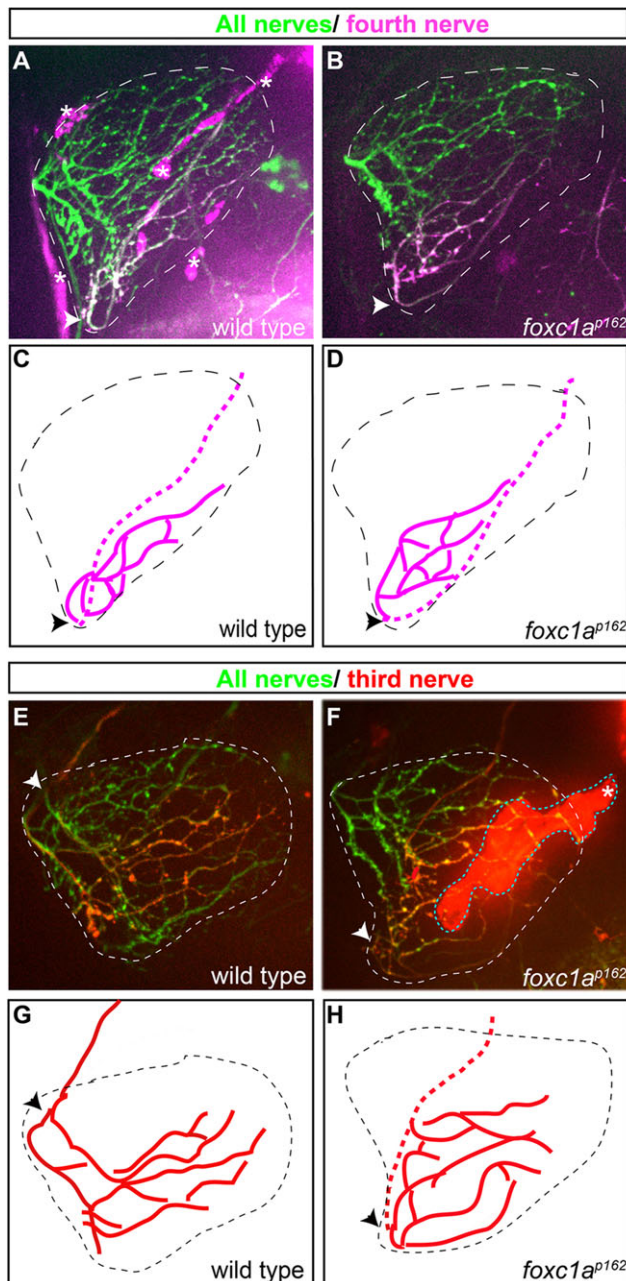


Fig. 5. Motor axons select their synaptic target independently of their migration history. (A-D) In wild type and *foxc1a* mutants, photoconverted Kik-GR-positive axons of the fourth fin nerve enter the fin at the ventral point of the fin and project to their ventroposterior target area. Arrowheads indicate where the nerve enters the fin. (E-H) In *foxc1a* mutants, photoconverted Kik-GR-positive axons of the third fin nerve enter the fin at an ectopic, ventral point of the fin yet project to the same target area as the corresponding wild-type axons that entered through the endogenous dorsal fin entry point. Red and magenta lines show tracing of photoconverted third and fourth nerves, respectively. Dotted lengths of red and magenta lines denote regions of the nerve underneath the fin. Asterisks (in A and F) and cyan dashed area (F) mark non-neural tissues giving background fluorescence in red channel. Scale bar: 50 μ m.

***foxc1a* mutants display defects in pectoral fin movement**

To examine whether the overall reduction in pectoral fin synapses observed in *foxc1a* mutants has functional consequences, we embedded 96-hpf-old zebrafish larvae with their fins able to move freely, and used a high-speed camera (200 frames/second) to record

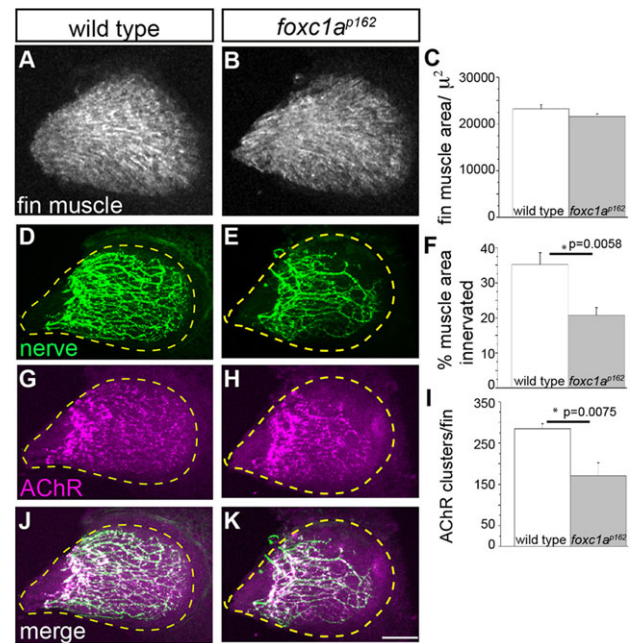


Fig. 6. *foxc1a* mutants display reduced fin nerve arborization and synaptic contacts. (A-C) At 96 hpf, fin muscle differentiation and surface area are unaffected in *foxc1a* mutants compared with wild type. (D-K) By contrast, the area of the fin muscle covered by presynaptic nerve branches (D-F) and the density of postsynaptic AChR clusters is significantly reduced in *foxc1a* mutants. All images are maximum projection views. The fin is outlined using a dashed yellow line. Scale bar: 50 μ m. (C,F,I) Asterisks indicate $P < 0.05$ (Student's *t*-test). Data are mean \pm s.e.m.

spontaneous fin movements. From these high-speed video recordings we calculated the amplitude of fin movements as the difference between the largest angle during the upward stroke (i.e. away from the body, angle X in Fig. 7C,D) and the smallest angle during the downward stroke (i.e. towards the body, angle Y in Fig. 7C,D). This kinematic analysis revealed that compared with wild-type animals both the mean fin-beating amplitude and the mean fin-beating frequency in *foxc1a* mutants are significantly reduced (Fig. 7E,F; $n=9$ fins from five animals for each genotype). Thus, *foxc1a* plays a crucial role in the development of appendage-specific neural circuits that drive appendage motility.

DISCUSSION

foxc1 encodes a transcription factor with well-defined roles in a wide range of developmental processes, including cerebellar, eye, vascular and organ development (Aldinger et al., 2009; Komaki et al., 2013; Kume et al., 2001; Seo and Kume, 2006; Seo et al., 2012; Sowden, 2007). In zebrafish, morpholino knockdown of *foxc1a* has been reported to cause defects in angioblast development (Veldman and Lin, 2012), and defects in eye vascularization (Skarie and Link, 2009). In a forward genetic screen for axonal guidance mutants, we identify a presumptive null allele in the zebrafish *foxc1a* gene, and demonstrate a previously unknown role of *foxc1a* as a key regulator to establish functional connectivity between the spinal cord and pectoral fins. Although transcription factors are known to control neuron intrinsic programs that also regulate growth cone behaviors, we find that *foxc1a* acts in the environment, in muscle cells along the axonal path towards the plexus region. Furthermore, we demonstrate that loss of *foxc1a* in muscle cells does not alter their identity. Instead, we propose that *foxc1a* expression in muscle cells generates a microenvironment selective

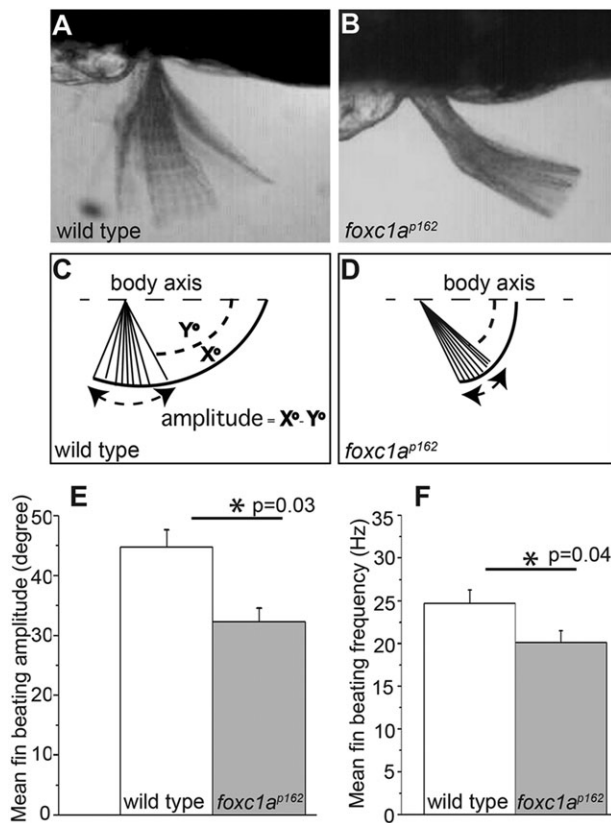


Fig. 7. *foxc1a* mutants exhibit reduced fin mobility. (A,B) Time projections from high-speed video recordings of 96 hpf wild type and *foxc1a* mutants reveal reduced pectoral fin mobility. (C,D) To quantify the defects, we defined the fin-beating amplitude as X° - Y° , where X° designates the maximum elevation angle of fin with respect to body axis (dashed line) in a given beating cycle, and Y° denotes the maximum depression angle in a given beating cycle. (E,F) *foxc1a* mutants display a significant reduction of both beating amplitude and frequency of pectoral fins. (C,F,I) Asterisks indicate $P < 0.05$ (Student's *t*-test).

for fin innervating nerves to promote their convergence to the plexus region at the base of the fin.

***foxc1a* defines a novel neuron extrinsic program selective for pectoral fin innervation**

Motor behaviors depend on precise connections between spinal motor neurons and their appropriate muscle targets, and one of the most complex sets of neuromuscular connections is the vertebrate limb. This is in part because the limb contains dozens of anatomically and functionally distinct muscle groups, and in part because, compared with axial motor axons, limb-innervating motor axons are confronted with additional guidance decision even before reaching the limb (Dasen and Jessell, 2009). Work over the past decade has identified a sequential motor neuron intrinsic transcriptional program that governs limb innervation. For example, motor neurons at limb levels of the spinal cord express the LIM homeodomain gene *Lhx3*, which directs their axons dorsally toward axial muscle, or express *Foxp1*, which directs their axons ventrally towards the limb (Dasen et al., 2008; Polleux et al., 2007; Rouso et al., 2008; Shirasaki et al., 2006). Similarly, guidance at the base of the limb to project dorsally or ventrally within the limb is also established by the differential expression of neuron intrinsic LIM homeodomain genes that then control the selective expression of guidance receptors (Bonanomi and Pfaff, 2010).

By contrast, the molecular program that controls axonal behaviors between their exit from the spinal cord en route to the limb and their entrance into the limb is not well understood. Between these two points, several segmental nerves converge at a defined area to form a plexus where axons mingle and then emerge to enter the limb. We find that *foxc1a* is dispensable for all aspects of axial motor axon guidance but is selectively required to guide pectoral fin-innervating motor axons, enabling the fin-innervating nerves to convergence onto a common plexus. In fact, their unique projection pattern suggests that fin nerves are dependent on guidance mechanisms that are distinct from those used by axial muscle motor nerves. Consistent with this, zebrafish mutants in which axial motor axon guidance is perturbed, display normal pectoral nerve projections (Palaisa and Granato, 2007; Zeller and Granato, 1999; Zeller et al., 2002; Zhang and Granato, 2000; Zhang et al., 2004).

foxc1a expression is strongly enriched in the somitic segments through which fin-innervating axons migrate where it functions cell non-autonomously in somitic muscle cells that delineate the axonal path towards the plexus. So how does *foxc1a* control axon guidance? One possible mechanism is that *foxc1a* regulates the expression of extracellular matrix (ECM) components or guidance cues in anterior somitic segments, thereby enabling axons to converge properly towards a plexus. For example, the secreted semaphorin Sema 3A, through its neuropilin 1 receptor, is thought to act through a 'surround repulsion' mechanism to maintain fasciculation as limb-innervating axons grow towards the plexus (Huber et al., 2005). Our RNA-seq analysis of anterior somitic segments did not identify ECM or 'classical' axonal guidance cues to be regulated by *foxc1a*, and in fact only identified 12 genes downregulated in *foxc1a* mutants. Among these downregulated genes, several (*foxd5*, *wnt8-2*, *sgcg*, *mybpha*) have been implicated in muscle patterning and structure (Klinge et al., 2008; Lee et al., 2009; Lekven et al., 2001). However, we did not find any gross patterning or structural muscles defects (Fig. 1 and supplementary material Fig. S2) in *foxc1a* mutants, confirming that the axonal defects in *foxc1a* mutants are not secondary, e.g. to the loss of muscle cell identity or integrity. Instead they suggest that *foxc1a* regulates the localization and/or stability of ECM molecules or guidance cues in the local nerve environment in a manner too subtle for detection at the transcriptional level. Importantly, many neuron-intrinsic transcription factors that establish wiring specificity have been identified over the past decade, yet the identification of relevant target genes still remains a challenge (Santiago et al., 2014). The application of recent technological advancements that allows transcriptional and translational profiling of individual muscle cells will be required to identify *foxc1a*-dependent genes relevant for motor axon guidance.

The role of the fin plexus for axonal targeting

Before entering the developing limb, limb innervating spinal nerves converge from adjacent spinal cord segments at the plexus. Previous studies revealed important roles for the plexus region in guiding axons to their designated muscle domains (Huber et al., 2005; Landmesser et al., 1990; Tang et al., 1992, 1994), yet its functional requirement in target selection is not clear. Like the limb nerves of birds and mammals, in zebrafish the first three fin nerves converge into the plexus at the base of the pectoral fin. In this study, we tested whether fin nerves that migrate through the plexus are dependent on plexus-derived signals to innervate their appropriate fin muscle targets. We find that, in *foxc1a* mutants, pectoral fin nerves bypassing the plexus enter the fin in an ectopic position, yet

innervate the designated muscle target within the fin, suggesting that plexus-independent cues within the fin contribute to the selection of final muscle target. The fact that, despite taking an aberrant route, the nerve still finds its designated muscle domain suggests signaling pathways implicated in nerve-muscle matching such as Ephrin signaling (Feng et al., 2000; Lampa et al., 2004) are still sufficiently operational in *foxc1a* mutants to direct fin nerves to their designated target muscles. This is consistent with the fact that, even in wild-type zebrafish, the fourth pectoral fin-innervating nerve selects its target domain without entering the plexus (Thorsen and Hale, 2007).

Why, then, do three of the four fin-innervating nerves converge at the plexus before entering the fin? Although migration through the plexus is not a prerequisite for target selection, it might enhance the efficacy of functional innervation by ensuring high axonal density in the fin. Consistent with this, we find that in *foxc1a* mutant fins, axonal branching and synaptic contact sites are reduced (Fig. 6). Although *foxc1a* expression is not detectable in the fin, it is possible that *foxc1a* promotes axonal arborization once axons enter the fin. Nonetheless, it is tempting to speculate that migration through the plexus promotes axonal entry into the fin and/or enhances innervation. Finally, although the precise mechanism by which *foxc1a* controls pectoral fin nerve guidance still remain to be defined, we propose that by generating a microenvironment that promotes the convergence of fin-innervating nerves into a plexus, *foxc1a* plays a specific and crucial role for the development of appendage-specific neural circuits that drive appendage motility.

MATERIALS AND METHODS

Ethics statement

All experiments were performed according to an Animal Protocol approved by the University of Pennsylvania Institutional Animal Care and Use Committee (IACUC) on 1/24/2014, protocol number 803446. Veterinary care is under the supervision of the University Laboratory Animal Resources (ULAR) of the University of Pennsylvania.

Zebrafish genetics

All embryos and larvae used in this study were raised at 28°C for the required amount of time (see Mullins et al., 1994). For all experiments, we used the *foxc1a*^{p162} mutant allele (referred as *foxc1a* mutant throughout the text and as *foxc1a*^{p162} in figures) in the TLF background. *Tg(mnx1:GFP)ml2* and *Tg(mnx1:Kik-GR)*^{p163} transgenic fish were either used alone, in combination with each other, or in combination with *foxc1a* mutants.

Molecular biology

foxc1a full-length cDNA was isolated from 28 hpf zebrafish embryos and cloned into pTOPO vector. The *foxc1a* cDNA was then cloned into *Bam*HI and *Xho*I sites of pCS2+ using the following primers (forward, 5'GAGGGATCCGGAGTTGTGTGGAGAGCAGT; reverse, 5'GACTCGAGGAACGGAGGAAAAATCAAGA). The *foxc1a*^{Δ118–476-myc} construct (i.e. the *foxc1a*^{p162} allele) was generated by amplifying the coding region preceding the stop codon in the *foxc1a*^{p162} allele using the following primers (forward, 5'AAGAATTCTTCTTGACGACTGTTCTTCGC; reverse, 5'AACCCGGGGCCCTGCTTGTGTCTCTGTAA). The DNA fragment was cloned into the *Eco*RI, *Xma*I site of the pCS2+myc vector to generate pCS2_{foxc1a}^{Δ118–476-myc}. To generate *actin:foxc1a-p2a-mKate*, *foxc1a* was first amplified with the following primers (forward, 5'ATCGCGGCCCGCTGGGAGTTGTGTGGAGAG; reverse, 5'GAGGGATCCAAATTTGCTGCAGTCATACA), and the resulting PCR fragment cloned into the *Not*I/*Bam*HI sites of a pEntry vector containing *p2a-mKate* to generate pEntry *foxc1a-p2a-mKate*. This was combined with the pDest-*α-actin* promoter (Higashijima et al., 1997) using LR cloning to generate mTol2 *α-actin:foxc1a-p2-mKate*. The ISceI:*mnx1:Kik-GR* construct was made by cloning *Kik-GR* (Tsutsui et al., 2005) into the *Bam*HI and *Xba*I site of a ISceI:*mnx1* vector.

Microinjection

DNA containing *α-actin:foxc1a-p2a-mKate* in the mini Tol2 vector was microinjected with transposon mRNA into the one-cell-stage zebrafish embryo as described by Kwan and colleagues (2007).

DNA extraction and library preparation for whole-genome sequencing

For whole-genome sequencing library preparation, 1–1.5 μg genomic DNA was sheared to 400 bp fragments using a Covaris sonicator. Sequencing library for the Illumina platform were prepared according to manufacturer's protocol using the Illumina low-throughput library preparation kit.

Whole-genome sequencing and SNP calling

Paired-end 100 bp high-throughput sequencing was performed on the Illumina HiSeq 2000 platform. The variants were called by applying best practices described in the GATK recommendations (DePristo et al., 2011; McKenna et al., 2010; Van der Auwera et al., 2013), which involved aligning the reads to the Zv9/danRer7 genome, and using the Burrows-Wheeler Aligner (BWA) (Li and Durbin, 2009) to map sequences. Variations not present in at least five read pairs were rejected from further analysis. Variants were characterized for their potential to damage protein function with SnpEff (Cingolani et al., 2012). Gene annotations were obtained from RefSeq (<http://www.ncbi.nlm.nih.gov/refseq/>) and Ensemble (<http://www.ensembl.org/index.html>).

RNA extraction and RNA sequencing

For RNA-seq, mRNA was extracted from 38–40-hpf embryos. We isolated wild-type and *foxc1a* mutant samples by dissecting the entire first six anterior somitic segments (AS) through which the fin nerves migrate, and the adjacent posterior segments (PS; segments 7 to ~12) devoid of fin-innervating nerves. Heads and yolks were excluded from all samples. Tissues were stored in RNAlater solution (Life Technologies) for up to 2 days at 4°C before RNA was extracted using the RNeasy kit (Qiagen) according to the manufacturer's protocol. RNA was tested for integrity using a Bioanalyzer (Agilent Technologies). RNA samples showing RIN value of eight or higher were used for generating cDNA libraries as described in the TruSeq Stranded mRNA sample preparation guide. At the final stage, 15 cycles of PCR amplifications were performed. Barcoded libraries representing duplicates of AS and PS samples of wild type and mutants were validated using Bioanalyzer (Agilent Technologies) and finally sequenced in Illumina HiSeq 2500 yielding paired end reads of 100 bp. The RNA-seq Unified Mapper (RUM) (Grant et al., 2011) was used to align the reads to the Zv9/danRer7 reference genome and to assign each read uniquely to a transcript. We investigated transcripts that showed the highest fold changes of expression between the different groups. For Gene Ontology annotations, genes tagged by the GO term 'axon guidance' were obtained from the gene ontology database (<http://www.geneontology.org/>). Next, we filtered this list for the 'Danio rerio' taxon (resulting in 116 unique genes) and used them to annotate our RNA-seq results. A full description of these data can be found at <http://www.ncbi.nlm.nih.gov/geo/query/acc.cgi?acc=GSE64125>.

Quantitative RT PCR

RNA samples were prepared in the same manner as described above for RNA-sequencing experiments using RNeasy kit (Qiagen), and were converted into cDNA using Superscript II kit (Life Technologies). qRT-PCRs were performed using the SYBR Green JumpStart qPCR mix (Sigma-Aldrich). The Ct (cycle threshold) values of the target genes (*mybpha*, *grapb*) in AS and PS samples were normalized to Ct values of *efl1a11* gene (housekeeping gene) in the AS and PS samples, respectively.

Immunohistochemistry

Antibody staining was performed as described previously (Zeller et al., 2002). The following primary antibodies were used: znp-1 (1:200) (Trevarrow et al., 1990), Antibody Facility, University of Oregon; SV2 (1:50), Developmental Studies Hybridoma Bank (DSHB), University of Iowa; MF20 (1:20, DSHB); F59 (1:20, DSHB); Engrailed/4D9 (1:5,

DSHB); anti rabbit GFP (1:400, Life Technologies); Alexa 594-coupled α -bungarotoxin (10 μ g/ml, Molecular Probes). Antibodies were visualized with Alexa-Fluor-488, Alexa-Fluor-594 and Alexa-Fluor-633-conjugated secondary antibodies (1:400, Molecular Probes). *In situ* hybridization was performed as previously described (Odenthal and Nusslein-Volhard, 1998). TUNEL staining was performed as previously described (Lowery and Sive, 2005) using Apoptag Peroxidase *In Situ* Apoptosis Detection Kit (Chemicon Cat# S7100). Anti-DIG-POD antibody (Roche) and Tyramide Signal Amplification (PerkinElmer) were used to detect TUNEL-positive nuclei (Gyda et al., 2012).

mRNA injections

mRNA was transcribed from linearized expression constructs using the SP6 mMessage mMachine kit (Ambion). mRNA was diluted in DEPC-water plus 0.5% Phenol Red. All embryos were injected at the one-cell stage with ~20 pg of wild-type *foxc1a* mRNA and 200 pg of *foxc1a* ^{Δ 118-476} *myc* mRNA.

Imaging

Embryos/larvae of desired age were mounted in Vectashield (Vector Labs) and imaged using 10 \times , 20 \times and 40 \times lenses using either a Spinning disk (Olympus) or a laser scanning confocal (Zeiss, LSM10) microscope. Appropriate numbers of z-sections were used to create maximum intensity projection image using Slidebook (3i) or NIH ImageJ/Fiji. Images were further processed using ImageJ and/or Photoshop. Images in Fig. 1A and Fig. 3A were created by stitching multiple xy-plane images spanning the whole embryo. Final versions of the figures for the manuscript were prepared using Adobe Illustrator. Live imaging was performed as previously described (Banerjee et al., 2011, 2013).

Photoconversion of Kik-GR protein

Transgenic larvae expressing the Kik-GR protein in motor neurons [*Tg(mnx1:Kik-GR)*] were anesthetized using tricane and mounted in 1.2% low melt agarose in Ringer's solution. Motor neuron cell bodies of a given fin nerve expressing the Kik-GR protein were then converted from green to red using the UV line of standard Zeiss Axioscope microscope. Larvae were subsequently released from the agar. At least 6 h were given to allow the photoconverted red Kik-GR protein to spread through the entire axon of the converted neurons. Larvae were then mounted again and imaged for fin nerve targeting.

Quantification of nerve branching and AChR clusters

All imaging for the fin nerve branching analysis was performed using identical acquisition parameter in LSM10 (Zeiss). Images were analyzed by Fiji (ImageJ). Briefly, we converted maximum projection images into binary images, and muscle area was outlined and calculated. In the same stack the total axonal branching area was calculated in the axonal channel of the binary images by dividing the total Integrated Density with 255. For Synaptic AChR measurement, we first outlined the muscle area and performed background subtraction and mean noise reduction. Then we used the 'find maxima' command to count the number of AChR cluster and considered those as synaptic AChR clusters where we had axonal signal in the same spot. We found more than 95% of the total AChRs are synaptic in both wild type and mutants. Statistical analysis was performed using the Student's *t*-test.

Fin movement analysis

Five *foxc1a* mutant and five wild-type zebrafish larvae (96 hpf) were randomly selected, briefly anesthetized with tricane and mounted in 1.2% low melt agar, keeping the pectoral fin exposed so that they could move freely. Larvae were allowed to recover for 15 min before recording spontaneous fin movements using a high-speed video camera (200 frames/second) mounted on a stereomicroscope. Each frame was analyzed manually, and a minimum intensity projection image was created for a given fin beating cycles (as shown in Fig. 7A,B). X and Y angles were calculated in Adobe illustrators. All statistical analysis was carried out using the Student's *t*-test.

Acknowledgements

We thank Dr M. Veldman for providing DNA constructs used in this study. We also thank members of the Granato laboratory for comments on the manuscript.

Competing interests

The authors declare no competing or financial interests.

Author contributions

S.B., J.B.H. and M.G. designed experiments; S.B. performed all experiments; S.B., K.H., J.B.H. and M.G. analyzed the data; and S.B. and M.G. wrote the manuscript with input from K.H. and J.B.H. All authors approved the final version of the manuscript.

Funding

This work is supported by grants to M.G. from the National Institutes of Health [NIH R01 HD37975 and NIH RO1 EY024861]. J.B.H. is supported by the National Institute of Neurological Disorders and Stroke [1R01NS054794-06], the Defense Advanced Research Projects Agency [DARPA-D12AP00025] and by the Penn Genome Frontiers Institute under a HRF grant with the Pennsylvania Department of Health. Deposited in PMC for release after 12 months.

Supplementary material

Supplementary material available online at <http://dev.biologists.org/lookup/suppl/doi:10.1242/dev.115816/-/DC1>

References

- Aldinger, K. A., Lehmann, O. J., Hudgins, L., Chizhikov, V. V., Bassuk, A. G., Ades, L. C., Krantz, I. D., Dobyns, W. B. and Millen, K. J. (2009). FOXC1 is required for normal cerebellar development and is a major contributor to chromosome 6p25.3 Dandy-Walker malformation. *Nat. Genet.* **41**, 1037–1042.
- Banerjee, S., Gordon, L., Donn, T. M., Berti, C., Moens, C. B., Burden, S. J. and Granato, M. (2011). A novel role for MuSK and non-canonical Wnt signaling during segmental neural crest cell migration. *Development* **138**, 3287–3296.
- Banerjee, S., Isaacman-Beck, J., Schneider, V. A. and Granato, M. (2013). A novel role for Lh3 dependent ECM modifications during neural crest cell migration in zebrafish. *PLoS ONE* **8**, e54609.
- Birely, J., Schneider, V. A., Santana, E., Dosch, R., Wagner, D. S., Mullins, M. C. and Granato, M. (2005). Genetic screens for genes controlling motor nerve-muscle development and interactions. *Dev. Biol.* **280**, 162–176.
- Bonanomi, D. and Pfaff, S. L. (2010). Motor axon pathfinding. *Cold Spring Harb. Perspect. Biol.* **2**, a001735.
- Cingolani, P., Platts, A., Wang, L. L., Coon, M., Nguyen, T., Wang, L., Land, S. J., Lu, X. and Ruden, D. M. (2012). A program for annotating and predicting the effects of single nucleotide polymorphisms, SnpEff: SNPs in the genome of *Drosophila melanogaster* strain w1118; iso-2; iso-3. *Fly (Austin)* **6**, 80–92.
- Dasen, J. S. and Jessell, T. M. (2009). Hox networks and the origins of motor neuron diversity. *Curr. Top. Dev. Biol.* **88**, 169–200.
- Dasen, J. S., De Camilli, A., Wang, B., Tucker, P. W. and Jessell, T. M. (2008). Hox repertoires for motor neuron diversity and connectivity gated by a single accessory factor, FoxP1. *Cell* **134**, 304–316.
- DePristo, M. A., Banks, E., Poplin, R., Garimella, K. V., Maguire, J. R., Hartl, C., Philippakis, A. A., del Angel, G., Rivas, M. A., Hanna, M. et al. (2011). A framework for variation discovery and genotyping using next-generation DNA sequencing data. *Nat. Genet.* **43**, 491–498.
- Eberhart, J., Swartz, M., Koblar, S. A., Pasquale, E. B., Tanaka, H. and Krull, C. E. (2000). Expression of EphA4, ephrin-A2 and ephrin-A5 during axon outgrowth to the hindlimb indicates potential roles in pathfinding. *Dev. Neurosci.* **22**, 237–250.
- Eberhart, J., Swartz, M. E., Koblar, S. A., Pasquale, E. B. and Krull, C. E. (2002). EphA4 constitutes a population-specific guidance cue for motor neurons. *Dev. Biol.* **247**, 89–101.
- Feng, G., Laskowski, M. B., Feldheim, D. A., Wang, H., Lewis, R., Frisen, J., Flanagan, J. G. and Sanes, J. R. (2000). Roles for ephrins in positionally selective synaptogenesis between motor neurons and muscle fibers. *Neuron* **25**, 295–306.
- Ferguson, B. A. (1983). Development of motor innervation of the chick following dorsal-ventral limb bud rotations. *J. Neurosci.* **3**, 1760–1772.
- Ferns, M. J. and Hollyday, M. (1993). Motor innervation of dorsoventrally reversed wings in chick/quail chimeric embryos. *J. Neurosci.* **13**, 2463–2476.
- Grant, G. R., Farkas, M. H., Pizarro, A. D., Lahens, N. F., Schug, J., Brunk, B. P., Stoeckert, C. J., Hogenesch, J. B. and Pierce, E. A. (2011). Comparative analysis of RNA-Seq alignment algorithms and the RNA-Seq unified mapper (RUM). *Bioinformatics* **27**, 2518–2528.
- Gyda, M., Wolman, M., Lorent, K. and Granato, M. (2012). The tumor suppressor gene retinoblastoma-1 is required for retinotectal development and visual function in zebrafish. *PLoS Genet.* **8**, e1003106.

- Higashijima, S.-i., Okamoto, H., Ueno, N., Hotta, Y. and Eguchi, G. (1997). High-frequency generation of transgenic zebrafish which reliably express GFP in whole muscles or the whole body by using promoters of zebrafish origin. *Dev. Biol.* **192**, 289-299.
- Huber, A. B., Kania, A., Tran, T. S., Gu, C., De Marco Garcia, N., Lieberam, I., Johnson, D., Jessell, T. M., Ginty, D. D. and Kolodkin, A. L. (2005). Distinct roles for secreted semaphorin signaling in spinal motor axon guidance. *Neuron* **48**, 949-964.
- Kania, A. and Jessell, T. M. (2003). Topographic motor projections in the limb imposed by LIM homeodomain protein regulation of ephrin-A:EphA interactions. *Neuron* **38**, 581-596.
- Klinge, L., Dekomien, G., Aboumoussa, A., Charlton, R., Epplen, J. T., Barresi, R., Bushby, K. and Straub, V. (2008). Sarcoglycanopathies: can muscle immunoanalysis predict the genotype? *Neuromuscul. Disord.* **18**, 934-941.
- Komaki, F., Miyazaki, Y., Niimura, F., Matsusaka, T., Ichikawa, I. and Motojima, M. (2013). Foxc1 gene null mutation causes ectopic budding and kidney hypoplasia but not dysplasia. *Cells Tissues Organs* **198**, 22-27.
- Kume, T., Jiang, H., Topczewska, J. M. and Hogan, B. L. M. (2001). The murine winged helix transcription factors, Foxc1 and Foxc2, are both required for cardiovascular development and somitogenesis. *Genes Dev.* **15**, 2470-2482.
- Kwan, K. M., Fujimoto, E., Grabher, C., Mangum, B. D., Hardy, M. E., Campbell, D. S., Parant, J. M., Yost, H. J., Kanki, J. P. and Chien, C.-B. (2007). The Tol2kit: a multisite gateway-based construction kit for Tol2 transposon transgenesis constructs. *Dev. Dyn.* **236**, 3088-3099.
- Lampa, S. J., Potluri, S., Norton, A. S., Fusco, W. and Laskowski, M. B. (2004). Ephrin-A5 overexpression degrades topographic specificity in the mouse gluteus maximus muscle. *Brain Res. Dev. Brain Res.* **153**, 271-274.
- Lance-Jones, C. and Landmesser, L. (1981). Pathway selection by embryonic chick motoneurons in an experimentally altered environment. *Proc. R. Soc. Lond. B Biol. Sci.* **214**, 19-52.
- Landmesser, L., Dahm, L., Tang, J. and Rutishauser, U. (1990). Polysialic acid as a regulator of intramuscular nerve branching during embryonic development. *Neuron* **4**, 655-667.
- Lee, H.-C., Tseng, W.-A., Lo, F.-Y., Liu, T.-M. and Tsai, H.-J. (2009). FoxD5 mediates anterior-posterior polarity through upstream modulator Fgf signaling during zebrafish somitogenesis. *Dev. Biol.* **336**, 232-245.
- Lekven, A. C., Thorpe, C. J., Waxman, J. S. and Moon, R. T. (2001). Zebrafish *wnt8* encodes two *wnt8* proteins on a bicistronic transcript and is required for mesoderm and neuroectoderm patterning. *Dev. Cell* **1**, 103-114.
- Li, H. and Durbin, R. (2009). Fast and accurate short read alignment with Burrows-Wheeler transform. *Bioinformatics* **25**, 1754-1760.
- Lowery, L. A. and Sive, H. (2005). Initial formation of zebrafish brain ventricles occurs independently of circulation and requires the *nanog* and *snakehead/atp1a1a.1* gene products. *Development* **132**, 2057-2067.
- Luria, V., Krawchuk, D., Jessell, T. M., Laufer, E. and Kania, A. (2008). Specification of motor axon trajectory by ephrin-B:EphB signaling: symmetrical control of axonal patterning in the developing limb. *Neuron* **60**, 1039-1053.
- Ma, L.-H., Gilland, E., Bass, A. H. and Baker, R. (2010). Ancestry of motor innervation to pectoral fin and forelimb. *Nat. Commun.* **1**, 49.
- McKenna, A., Hanna, M., Banks, E., Sivachenko, A., Cibulskis, K., Kernytsky, A., Garimella, K., Altshuler, D., Gabriel, S., Daly, M. et al. (2010). The genome analysis toolkit: a MapReduce framework for analyzing next-generation DNA sequencing data. *Genome Res.* **20**, 1297-1303.
- Mullins, M. C., Hammerschmidt, M., Haffter, P. and Nüsslein-Volhard, C. (1994). Large-scale mutagenesis in the zebrafish: in search of genes controlling development in a vertebrate. *Curr. Biol.* **4**, 189-202.
- Murphy, T. C., Saleem, R. A., Footz, T., Ritch, R., McGillivray, B. and Walter, M. A. (2004). The wing 2 region of the FOXC1 forkhead domain is necessary for normal DNA-binding and transactivation functions. *Invest. Ophthalmol. Vis. Sci.* **45**, 2531-2538.
- Myers, P. Z. (1985). Spinal motoneurons of the larval zebrafish. *J. Comp. Neurol.* **236**, 555-561.
- Myers, P. Z., Eisen, J. S. and Westerfield, M. (1986). Development and axonal outgrowth of identified motoneurons in the zebrafish. *J. Neurosci.* **6**, 2278-2289.
- Nishimura, D. Y., Searby, C. C., Alward, W. L., Walton, D., Craig, J. E., Mackey, D. A., Kawase, K., Kanis, A. B., Patil, S. R., Stone, E. M. et al. (2001). A spectrum of FOXC1 mutations suggests gene dosage as a mechanism for developmental defects of the anterior chamber of the eye. *Am. J. Hum. Genet.* **68**, 364-372.
- Odenthal, J. and Nüsslein-Volhard, C. (1998). fork head domain genes in zebrafish. *Dev. Genes Evol.* **208**, 245-258.
- Palaisa, K. A. and Granato, M. (2007). Analysis of zebrafish sidetracked mutants reveals a novel role for Plexin A3 in intraspinal motor axon guidance. *Development* **134**, 3251-3257.
- Patterson, S. E., Mook, L. B. and Devoto, S. H. (2008). Growth in the larval zebrafish pectoral fin and trunk musculature. *Dev. Dyn.* **237**, 307-315.
- Pike, S. H., Melancon, E. F. and Eisen, J. S. (1992). Pathfinding by zebrafish motoneurons in the absence of normal pioneer axons. *Development* **114**, 825-831.
- Polleux, F., Ince-Dunn, G. and Ghosh, A. (2007). Transcriptional regulation of vertebrate axon guidance and synapse formation. *Nat. Rev. Neurosci.* **8**, 331-340.
- Rouso, D. L., Gaber, Z. B., Wellik, D., Morrisey, E. E. and Novitsch, B. G. (2008). Coordinated actions of the forkhead protein Foxp1 and Hox proteins in the columnar organization of spinal motor neurons. *Neuron* **59**, 226-240.
- Saleem, R. A., Banerjee-Basu, S., Murphy, T. C., Baxevanis, A. and Walter, M. A. (2004). Essential structural and functional determinants within the forkhead domain of FOXC1. *Nucleic Acids Res.* **32**, 4182-4193.
- Santiago, C., Labrador, J.-P. and Bashaw, G. J. (2014). The homeodomain transcription factor Hb9 controls axon guidance in Drosophila through the regulation of Robo receptors. *Cell Rep.* **7**, 153-165.
- Seo, S. and Kume, T. (2006). Forkhead transcription factors, Foxc1 and Foxc2, are required for the morphogenesis of the cardiac outflow tract. *Dev. Biol.* **296**, 421-436.
- Seo, S., Singh, H. P., Lecal, P. M., Sasman, A., Fatima, A., Liu, T., Schultz, K. M., Losordo, D. W., Lehmann, O. J. and Kume, T. (2012). Forkhead box transcription factor FoxC1 preserves corneal transparency by regulating vascular growth. *Proc. Natl. Acad. Sci. USA* **109**, 2015-2020.
- Shirasaki, R., Lewcock, J. W., Lettieri, K. and Pfaff, S. L. (2006). FGF as a target-derived chemoattractant for developing motor axons genetically programmed by the LIM code. *Neuron* **50**, 841-853.
- Skarke, J. M. and Link, B. A. (2009). FoxC1 is essential for vascular basement membrane integrity and hyaloid vessel morphogenesis. *Invest. Ophthalmol. Vis. Sci.* **50**, 5026-5034.
- Sowden, J. C. (2007). Molecular and developmental mechanisms of anterior segment dysgenesis. *Eye (Lond)* **21**, 1310-1318.
- Tang, J., Landmesser, L. and Rutishauser, U. (1992). Polysialic acid influences specific pathfinding by avian motoneurons. *Neuron* **8**, 1031-1044.
- Tang, J., Rutishauser, U. and Landmesser, L. (1994). Polysialic acid regulates growth cone behavior during sorting of motor axons in the plexus region. *Neuron* **13**, 405-414.
- Thorsen, D. H. and Hale, M. E. (2007). Neural development of the zebrafish (*Danio rerio*) pectoral fin. *J. Comp. Neurol.* **504**, 168-184.
- Tosney, K. W. and Landmesser, L. T. (1984). Pattern and specificity of axonal outgrowth following varying degrees of chick limb bud ablation. *J. Neurosci.* **4**, 2518-2527.
- Trevarrow, B., Marks, D. L. and Kimmel, C. B. (1990). Organization of hindbrain segments in the zebrafish embryo. *Neuron* **4**, 669-679.
- Tsutsui, H., Karasawa, S., Shimizu, H., Nukina, N. and Miyawaki, A. (2005). Semi-rational engineering of a coral fluorescent protein into an efficient highlighter. *EMBO Rep.* **6**, 233-238.
- Van der Auwera, G. A., Carneiro, M. O., Hartl, C., Poplin, R., del Angel, G., Levy-Moonshine, A., Jordan, T., Shakir, K., Roazen, D., Thibault, J. et al. (2013). From FastQ data to high-confidence variant calls: the genome analysis toolkit best practices pipeline. *Curr. Protoc. Bioinform.*
- Veldman, M. B. and Lin, S. (2012). *Etsrp/Etv2* is directly regulated by Foxc1a/b in the zebrafish angioblast. *Circ. Res.* **110**, 220-229.
- Weisschuh, N., Dressler, P., Schuettauf, F., Wolf, C., Wissinger, B. and Gramer, E. (2006). Novel mutations of FOXC1 and PITX2 in patients with Axenfeld-Rieger malformations. *Invest. Ophthalmol. Vis. Sci.* **47**, 3846-3852.
- Westerfield, M., McMurray, J. V. and Eisen, J. S. (1986). Identified motoneurons and their innervation of axial muscles in the zebrafish. *J. Neurosci.* **6**, 2267-2277.
- Yan, B., Neilson, K. M. and Moody, S. A. (2009). Notch signaling downstream of foxD5 promotes neural ectodermal transcription factors that inhibit neural differentiation. *Dev. Dyn.* **238**, 1358-1365.
- Zeller, J. and Granato, M. (1999). The zebrafish *diwanka* gene controls an early step of motor growth cone migration. *Development* **126**, 3461-3472.
- Zeller, J., Schneider, V., Malayaman, S., Higashijima, S.-i., Okamoto, H., Gui, J., Lin, S. and Granato, M. (2002). Migration of zebrafish spinal motor nerves into the periphery requires multiple myotome-derived cues. *Dev. Biol.* **252**, 241-256.
- Zhang, J. and Granato, M. (2000). The zebrafish unplugged gene controls motor axon pathway selection. *Development* **127**, 2099-2111.
- Zhang, J., Lefebvre, J. L., Zhao, S. and Granato, M. (2004). Zebrafish unplugged reveals a role for muscle-specific kinase homologs in axonal pathway choice. *Nat. Neurosci.* **7**, 1303-1309.